Chapter 7
Synthesis and Characterization of Ion-Implanted Epoxy Composites for X-Ray Shielding

Abstract The epoxy samples were implanted with heavy ions such as tungsten (W), gold (Au) and lead (Pb) to investigate the attenuation characteristics of these composites. Near-surface composition depth profiling of ion-implanted epoxy systems was studied using Rutherford Backscattering Spectroscopy (RBS). The effect of implanted ions on the X-ray attenuation was studied with a general diagnostic X-ray machine with X-ray tube voltages from 40 to 100 kV at constant exposure 10 mAs. Results show that the threshold of implanted ions above which X-ray mass attenuation coefficient, μ_m of the ion-implanted epoxy composite is distinguishably higher than the μ_m of the pure epoxy sample is different for W, Au and Pb.

7.1 Introduction

X-ray shielding requirements have become more stringent as standards for exposure of personnel and general public have been re-assessed. X-rays technologists practice the ALARA principle (as low-as-reasonably-achievable) dose when dealing with harmful ionizing radiation in order to continuously minimize the dose received by personnel and general public [1–5]. Moreover, the application of polymers in X-ray shielding technology is increasing steadily. This is due to a number of advantages such as the choice of fillers into the polymer matrix, the improved dispersion of fillers which enable the formation of mechanically stable hard coating materials and the possibility to modify both chemical composition and the related physical properties of polymers by easy-to-control fabrication parameters [6–11]. In addition, other surface modification tools such as ion implantation has also become increasingly used due to the ease and readability to process some parameters during the irradiation such as the choice of ions, the ion fluence, the depth of ion implantation, etc., which can further improve the X-ray absorption capacity of shielding materials, including polymers [7, 9, 12–14]. The main advantage of ion-implantation technology is the capability of accurately controlling the number of implanted dopant atoms and the dopant's depth distribution profile [15]. In addition, the ion-implantation is well established, and well understood technology as shown in applications for modifying the surface properties of metals, semiconductors and ceramics. More recently, the ion

I. M. Low and N. Z. Noor Azman, *Polymer Composites and Nanocomposites for X-Rays Shielding*, Composites Science and Technology,
https://doi.org/10.1007/978-981-13-9810-0_7

implantation technology has been applied to the surface modification of polymers to enhance their mechanical and electrical properties without changing the bulk properties [10, 11, 16–19]. Promising results on ion-implanted ultra high molecular weight polyethylene (UHMWPE) have been shown by Chen et al. where improved hardness and Young's modulus could be obtained through nitrogen ion-implantation [14]. In addition, an epoxy system is a thermoset polymer which is generally stronger and better suited to higher temperatures than thermoplastics so it can withstand the high energetic ion during the implantation process [20]. Hence, the purpose of the present study is to synthesize and characterize the X-ray attenuation property, microstructure and near-surface composition of epoxy composites which have been implanted with heavy ions such as tungsten (W), gold (Au) and lead (Pb).

7.2 Results and Discussion

7.2.1 Rutherford Backscattering Spectroscopy (RBS)

The RBS results in Fig. 7.1 shows the yield versus channel number for samples B1, B3 and B5 implanted with W, Au and Pb, respectively. The list of samples with the different amount of implanted ions is shown in Table 7.1. These results confirm that a higher nominal dose resulted in a higher implanted concentration in the samples. For example, for Au-implanted sample B3, a maximum Au concentration of 0.13 at.% has been implanted in epoxy down to a depth of about 600 mono layers (ML) and it

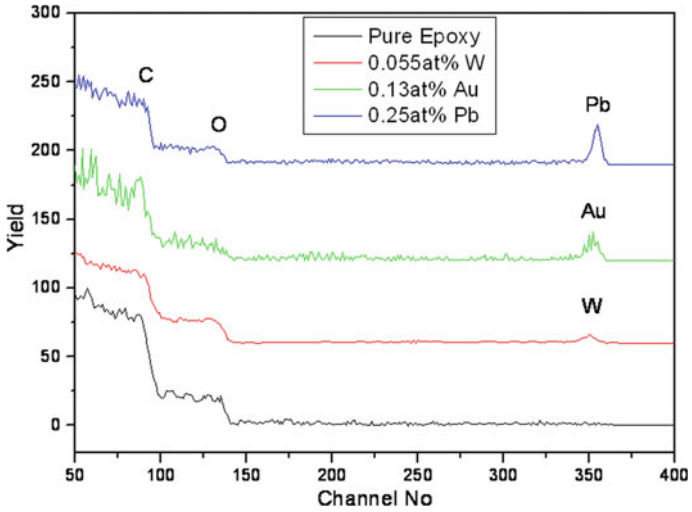

Fig. 7.1 RBS result for pure epoxy sample and implanted samples B1 (0.055 at.% W), B3 (0.13 at.% Au) and B5 (0.25 at.% Pb) [21]

Table 7.1 List of samples prepared with different implanted ions, average charge and RBS concentration of implanted ion

Sample ID	Implanted ion	Average charge	RBS concentration (at.%)
B1	W	+3.07	0.055
B2	W		0.115
B3	Au	+1.99	0.130
B4	Au		0.230
B5	Pb	+1.66	0.250
B6	Pb		0.402

drops to 0.06 at.% for the next 800 ML. For sample B4 a maximum Au concentration of 0.23 at.% has been implanted in epoxy down to a depth of about 700 ML and then it drops to about 0.08 at.% for the next 900 ML. This small difference in the implantation depth of Au in epoxy is attributed to the small differences in the local density of the hand-made epoxy polymer. A similar depth-profile RBS results was obtained for samples implanted with W and Pb.

7.2.2 X-Ray Mass Attenuation Coefficients

Figure 7.2 shows the mass attenuation coefficient, μ_m as a function of X-ray tube voltage for pure epoxy sample and for samples implanted with all three ions at various

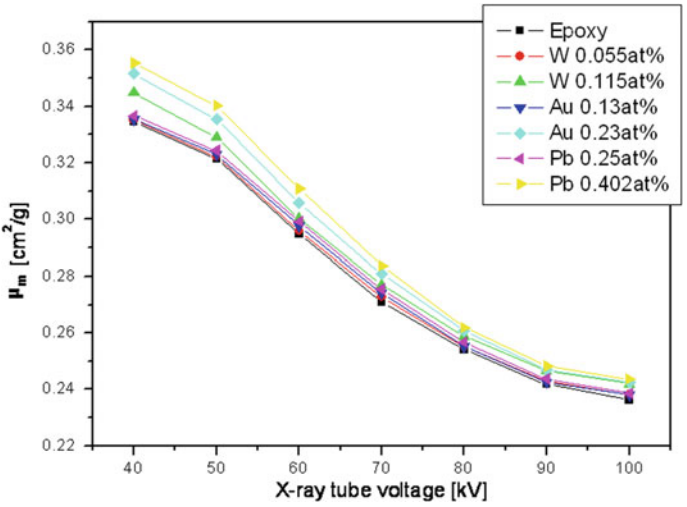

Fig. 7.2 Comparison of μ_m versus X-ray tube voltage for pure epoxy sample and all implanted samples [21]

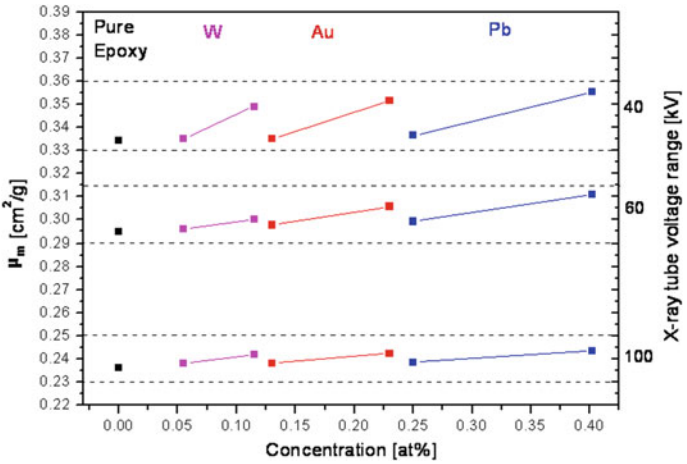

Fig. 7.3 Variation of μ_m with concentration of implanted ion, the type of implanted ion and the excitation energy of the X-ray tube [21]

concentrations, as determined by RBS. The results illustrate the typical decrease of μ_m with the increase of X-ray tube excitation voltage, due to a higher energy bremsstrahlung. In addition, a small increase of μ_m is noticed with the change of the implanted elements (W, Au and Pb). For small concentrations of implanted elements, the variation of μ_m with the X-ray tube voltage is similar with the result of μ_m for pure epoxy. However, for higher concentration of implanted elements, there is a noticeable increase of μ_m above the μ_m of pure epoxy, at each X-ray tube voltage, but this increase is higher at lower excitation voltages (energies). This is better illustrated in Fig. 7.3, where we capture the variation of μ_m with concentration of implanted ion, the type of implanted ion and the excitation energy of the X-ray tube. In addition, with the decreasing of μ_m with the increased of X-ray energy, we note the increase of μ_m with the concentration of implanted element and with type of implanted element. For the same energy of X-rays, the heavier the implanted ion or in other word the higher the atomic number of implanted ion, the higher is the value of μ_m. These were due to the photoelectric interaction that dominates in the low X-ray energy range and high atomic number of absorbing material. The probability of the photoelectric interaction is approximately dependent on Z^3/E^3 where Z is atomic number of the absorbing material (implanted ions) and E is the photon energy [22].

Figure 7.3 also shows that for the same excitation voltage, the increase of μ_m is more effective and that small additions of W afford a reasonable increase. For example (see Table 7.1) for comparable concentrations of 0.115 at.% W (sample B2) and 0.13 at.% Au (sample B3), the W appears to be more effective in increasing the μ_m which is contrary to what we expect since the atomic number of W is lower than the atomic number of Au. A possible explanation could be that at these concentrations, Au and Pb is agglomerating to a higher degree than W, but this is yet to be verified by cross section TEM. However, in terms of the relative increase in the concentration of

Table 7.2 Relative increase of μ_m with the excitation of the X-ray tube for a relative increase in the concentration of implanted ions of: W = 109.1%; Au = 76.9% and Pb = 60.8%

X-ray tube excitation voltage (kV)	W (%)	Au (%)	Pb (%)
40	4.18	4.95	5.55
60	1.45	2.69	3.01
100	1.64	1.59	2.09

implanted ions, the increase of μ_m is higher for Pb, as shown in Table 7.2. Table 7.2 also shows that within the range used for the excitation voltage of the X-ray tube, the doping threshold where μ_m of the composite starts to be larger than the μ_m of the pure epoxy is around 0.1 at.% for W, 0.2 at.% for Au and 0.25 at.% for Pb.

7.3 Conclusions

The ion-implantation technique has been successfully used to implant epoxy resin with W, Au and Pb at various concentrations, and the X-ray mass attenuation coefficient of the composite has been measured in a range of 40–100 kV of the excitation voltage for the X-ray tube. It has been shown that the threshold of implanted ions above which μ_m of the ion-implanted epoxy composite is distinguishably higher than the m of the pure epoxy is different for W, Au and Pb. The practical concentrations of W, Au and Pb in epoxy composite which could provide good X-ray attenuation properties and could be considered as candidates for effective X-ray shielding in diagnostic radiology is higher than the concentrations used in this report, and further work is considered.

Acknowledgements The work on ion-implantation and ion-beam analysis was conducted at the Australian Nuclear Science and Technology Organisation with financial support from AINSE under grant AINGRA 11-135.

References

1. Okunade AA (2002) Comparison of lead attenuation and lead hardening equivalence of materials used in respect of diagnostic X-ray shielding. Appl Radiat Isot 57:819–824
2. Okunade AA (2004) Numerical models for the determination of primary structural barriers for diagnostic X-ray facilities. Med Phys 31:513–520
3. Archer BR (2005) Recent history of the shielding of medical X-ray imaging facilities. Health Phys 88:579–586
4. Dixon RL, Simpkin DJ (1998) Primary shielding barriers for diagnostic X-ray facilities: a new model. Health Phys 74:181–189
5. Hessenbruch A (2002) A brief history of X-rays. Endeavour 26:137–141
6. Wu Y, Zhang T, Zhang H, Zhang X, Deng Z, Zhou G (2000) Electrical properties of polymer modified by metal ion implantation. Nucl Instrum Methods Phys Res, Sect B 169:89–93

7. Dworecki K, Drabik M, Hasegawa T, Wąsik S (2004) Modification of polymer membranes by ion implantation. Nucl Instrum Methods Phys Res, Sect B 225:483–488
8. Hubler GK (1981) Use of ion beam analysis in metal modification by means of ion implantation. Nucl Instrum Methods Phys Res 191:101–113
9. Soares MRF, Alegaonkar P, Behar M, Fink D, Muller M (2004) $^{6}Li^{+}$ ion implantation into polystyrene. Nucl Instrum Methods Phys Res, Sect B 218:300–307
10. Lee EH, Rao GR, Lewis MB, Mansur LK (1993) Ion beam application for improved polymer surface properties. Nucl Instrum Methods Phys Res, Sect B 74:326–330
11. Yuguang W, Tonghe Z, Huixing Z, Xiaoji Z, Zhiwei D (2000) Polymer modification by MEVVA source deposited and ion implantation. Surf Coat Technol 131:520–524
12. Lopatin CM, Alford TL, Pizziconi VB, Kuan M, Laursen T (1998) Ion-beam densification of hydroxyapatite thin films. Nucl Instrum Methods Phys Res, Sect B 145:522–531
13. Anders A (1997) Ion charge state distributions of vacuum arc plasmas: The origin of species. Phys Rev E 55:969
14. Chen JS, Lau SP, Sun Z, Tay BK, Yu GQ, Zhu FY, Zhu DZ, Xu HJ (2001) Structural and mechanical properties of nitrogen ion implanted ultra high molecular weight polyethylene. Surf Coat Technol 138:33–38
15. http://www.ece.gatech.edu/research/labs/vc/theory/ionimplant.html#depth, 22 June 2010
16. Kozlov EV, Ryabchikov AI, Sharkeev YP, Stepanov IB, Fortuna SV, Sivin DO, Kurzina IA, Prokopova TS, Mel'nik IA (2002) Formation of intermetallic layers at high intensity ion implantation. Surf Coat Technol 158–159:343–348
17. Evans PJ, Hyvarinen J, Samandi M (1995) Surface modification of austenitic stainless steel by titanium ion implantation. Surf Coat Technol 71:151–158
18. Ashworth V, Grant WA, Procter RPM, Wright EJ (1978) The effect of ion implantation on the corrosion behavior of pure iron-IV. Lead ion implantation. Corros Sci 18:681–685
19. Wang C, Tao YX (1985) The influence of boron ion-implantation on silica and lead glasses. J Non-Cryst Solids 71:397–402
20. Archos LLC. http://www.archos-llc.com/Material_Guide_2.html, 6 Oct 2011
21. Noor Azman NZ, Siddiqui SA, Ionescu M, Low IM (2012) Synthesis and characterisation of ion-implanted epoxy composites for X-ray shielding. Nucl Instrum Methods Phys Res, Sect B 287:120–123
22. Sprawls P (1993) The physical principles of medical imaging, 2nd edn. Aspen Publishers, Gaithersburg, MD